

Experimental signature of medium modifications for ρ and ω mesons in 12GeV p + A reaction

M. Naruki,^{*} Y. Fukao, H. Funahashi, M. Ishino,[†] H. Kanda,[‡] M. Kitaguchi,[§] S. Mihara,[†] K. Miwa, T. Miyashita, T. Murakami, T. Nakura, F. Sakuma, M. Togawa, S. Yamada,[¶] and Y. Yoshimura
Department of Physics, Kyoto University, Kitashirakawa Sakyo-ku, Kyoto 606-8502, Japan

H. En'yo, R. Muto, T. Tabaru, and S. Yokkaichi
RIKEN, 2-1 Hirosawa, Wako, Saitama 351-0198, Japan

J. Chiba,^{**} M. Ieiri, O. Sasaki, M. Sekimoto, and K. H. Tanaka
Institute of Particle and Nuclear Studies, KEK, 1-1 Oho, Tsukuba, Ibaraki 305-0801, Japan

H. Hamagaki and K. Ozawa
*Center for Nuclear Study, Graduate School of Science,
University of Tokyo, 7-3-1 Hongo, Tokyo 113-0033, Japan*
(Dated: February 9, 2020)

The invariant mass spectra of e^+e^- pairs produced in 12-GeV proton-induced nuclear reactions are measured at the KEK Proton Synchrotron. On the low-mass side of the ω meson peak, a significant enhancement over the known hadronic sources has been observed. The mass spectra, including the excess, are well reproduced by a model that takes into account the density dependence of the vector meson mass modification, as theoretically predicted.

PACS numbers: 14.40.Cs, 21.65.+f, 25.40.Ve, 24.85.+p

It is well established that most of hadron masses are generated due to the spontaneous breaking of the chiral symmetry, which is the crucial aspect of the strong interaction. The modification of hadron masses and decay widths in hot and/or dense matter is theoretically predicted as a consequence of the restoration of the broken symmetry. Experimental observations of such phenomena have become one of the most interesting topics in hadron physics today.

As for theoretical studies, many works have been performed and they are summarized in [1, 2]. Specifically, our experiment was motivated by two related studies concerning dense matter. Using an effective chiral Lagrangian, Brown and Rho proposed an in-medium scaling law, which predicted a decrease of the vector meson mass at 20% at the normal nuclear density ρ_0 [3, 4]. Hatsuda and Lee calculated the density dependence of the mass of vector mesons based on the QCD sum rule to reach the conclusion that the mass is approximately linear to the density in $0 < \rho < 2\rho_0$, and the mass of ρ and ω mesons decreases at about 16% at ρ_0 [5, 6].

The experiment E325 has been performed at the KEK 12-GeV Proton Synchrotron to measure the invariant mass spectra of $\rho, \omega, \phi \rightarrow e^+e^-$ and $\phi \rightarrow K^+K^-$ decay modes simultaneously. Our main goal is to detect the modification of the spectral shape of vector mesons in nuclear media. In our earlier publication, we showed the significant enhancement below the ω peak in the invariant mass spectrum of e^+e^- pairs for a copper target, which is attributed to the mass-modification effect in nuclear matter [7]. This was the first dilepton measurement of

the modification of the vector meson mass in nucleus.

It should be noted that our earlier and present results are strongly related to other few experimental observations. The CERES/NA45 collaboration observed the low-mass electron-pair enhancement in Pb-Au collisions at 158 A GeV [8]. The STAR collaboration reported the shift of ρ meson peak in the $\pi^+\pi^-$ channel at RHIC in Au+Au and p+p collisions at $\sqrt{s} = 200$ GeV/ c^2 [9]. Their results may connote the chiral symmetry restoration in hot matter. The TAGX collaboration reported an in-medium modification of the ρ invariant mass distribution via ${}^3\text{He}, {}^{12}\text{C}(\gamma, \pi^+\pi^-)X$ reactions [10]. Recently, the CBELSA/TAPS collaboration has reported that the mass modification of ω meson in the $\pi^0\gamma$ channel [11].

Although these diverse experimental signatures, including ours, are not ample, they could be related to a critical behavior of hadrons in hot and/or dense matter. Compared to other experiments, our experiment is unique, since we are able to measure the e^+e^- mass shapes directly with a high mass resolution and high statistics, placing a special emphasis on vector mesons that decay inside a nucleus. Needless to say, lepton pairs are almost free from final state interactions with nuclear matter.

The results presented in this paper are based on most of the data that we have acquired. The statistics have improved by about 50-times compared to those given in a previous paper [7]. We will show a comparison of the data to the theoretical prediction using a toy model dealing with the density dependence of the vector meson masses.

A detailed description of the E325 spectrometer can

be found elsewhere [12]. The detector elements, which are relevant for this analysis, are briefly discussed below. The spectrometer was designed to detect decays of slowly moving vector mesons, which have a larger probability to decay inside a target nucleus. In 2002, the primary proton beam with a typical intensity of 7×10^8 Hz was delivered to one carbon and four copper disk targets, which were aligned in-line along the beam axis. The interaction length of each copper target is 0.054%(73 mg/cm², 0.57% in radiation length), and that of the carbon target is 0.21%(184 mg/cm², 0.43% in radiation length). The tracking system, consists of three drift chambers, gives the momentum resolution of $\sigma_p/p = \sqrt{(1.37\% \cdot p)^2 + 0.41\%^2}$ [12].

The mass resolution and mass scale were examined for the observed peaks of $\Lambda \rightarrow p\pi^-$ and $K_s^0 \rightarrow \pi^+\pi^-$ decays. The observed resolutions and centroids of these resonances are consistent with the expectations given by a detailed detector simulation using Geant4 [13]. The effects caused by multiple scattering, energy losses, the chamber resolution, and a miss-alignment of the tracking devices were minutely inspected. Please note that the mass spectra presented in this manuscript is not corrected for the mass scale which is 3.7 ± 0.8 MeV/c² lower than the real value at 0.8 GeV/c² (i.e. ω peak). At the low-mass side of the resonances, a long tail arises due to the energy loss of electrons, mainly caused by bremsstrahlung. Such a tail is estimated to be negligible compared to the excess that we have been observing. The mass resolutions for $\omega \rightarrow e^+e^-$ and $\phi \rightarrow e^+e^-$ decays are estimated to be 8.0 and 10.7 MeV/c², respectively. These values are consistent with the data when we neglected the excess parts of the mass spectra.

Figure 1 shows the invariant mass spectra of the e^+e^- pairs using all of the data taken in 2002. We have required each track of an e^+e^- pair to come into each of the two arms; therefore, the low-mass region of the spectra is largely suppressed. The invariant mass spectra was fitted with the combinatorial background and known hadronic sources: $\rho \rightarrow e^+e^-$, $\omega \rightarrow e^+e^-$, $\phi \rightarrow e^+e^-$, $\eta \rightarrow e^+e^-\gamma$, and $\omega \rightarrow e^+e^-\pi^0$. The combinatorial background was evaluated by the event-mixing method. The relativistic Breit-Wigner distribution was used to obtain the spectral shapes of resonances. The mass resolution and the detector effect of our spectrometer were taken into account through the detector simulation described before. The kinematical distributions of mesons have been obtained by the nuclear cascade code JAM [15], which is in a good agreement with the real data. The relative abundances of these components were determined by the fitting, except for the ratio of $\omega \rightarrow e^+e^-\pi^0$ to $\omega \rightarrow e^+e^-$ decay which was fixed to their branching ratios, 59/6.95 given by the PDG [16]. The fit results are plotted with the solid lines in Fig.1 and summarized in Table I. The obtained $\chi^2/d.o.f.$ are 161/140 and 154/140 for the C and Cu targets, respectively. The region from 0.6 to 0.76 GeV/c²

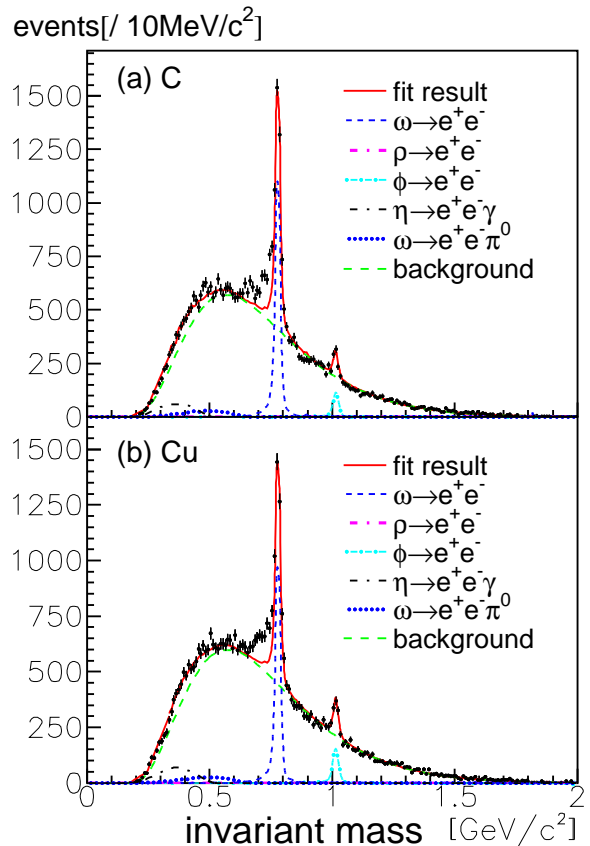


FIG. 1: Invariant mass spectra of e^+e^- for the (a) C and (b) Cu targets. The solid lines are the best-fit results, which is the sum of the known hadronic decays, $\omega \rightarrow e^+e^-$ (dashed), $\phi \rightarrow e^+e^-$ (thick dash-dotted), $\eta \rightarrow e^+e^-\gamma$ (dash-dotted), and $\omega \rightarrow e^+e^-\pi^0$ (dotted) together with the combinatorial background (long-dashed). $\rho \rightarrow e^+e^-$ is not visible (see text).

TABLE I: Signal yields in the acceptance together with $\chi^2/d.o.f.$ for the C and Cu targets, obtained by the fit excluding the mass range of 0.6 to 0.76 GeV/c². The values for ρ are expressed as an upper limit at 95% C.L.

	η Dalitz	ϕ	ω	ρ	excess	χ^2/dof
C	1012 \pm 112	398 \pm 42	3644 \pm 92	(112)	1461 \pm 131	161/140
Cu	1249 \pm 126	547 \pm 45	3346 \pm 91	(169)	1341 \pm 136	154/140

TABLE II: Same as Table I but corresponds to the fit including the excess region.

	η Dalitz	ϕ	ω	ρ	excess	χ^2/dof
C	1025 \pm 116	347 \pm 40	3552 \pm 98	1468 \pm 242	893 \pm 169	366/162
Cu	1248 \pm 132	505 \pm 44	3209 \pm 98	1405 \pm 257	798 \pm 175	295/162

was excluded from the fit, because the fit including this region resulted in failure at C.L. 99.9% as listed in Table II [28].

A significant excess can be seen on the low-mass side of the ω peak, whereas the high-mass tail of the ω can be reproduced with the expected shapes. The number

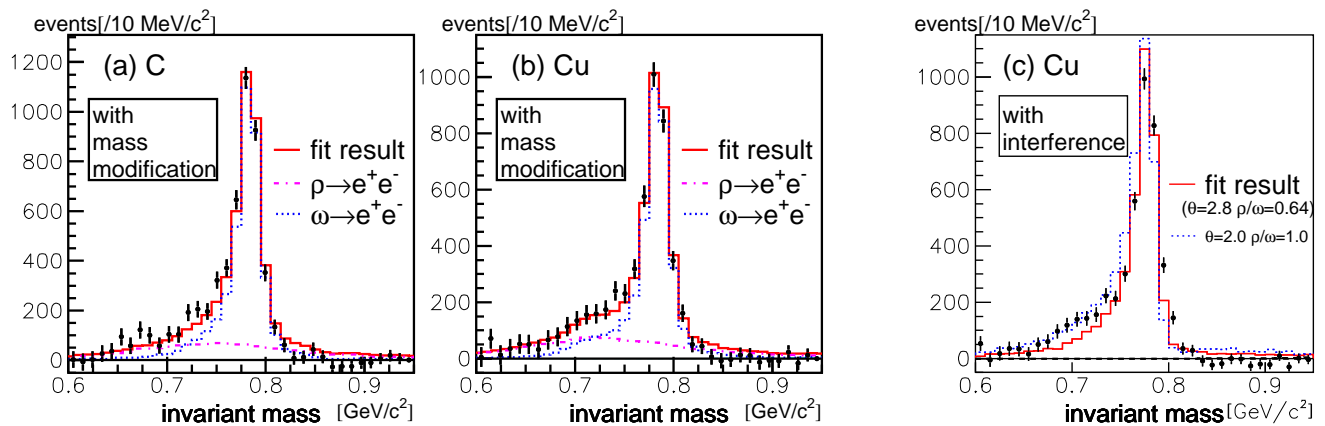


FIG. 2: Invariant mass spectra of e^+e^- . The combinatorial background and the shapes of $\eta \rightarrow e^+e^-\gamma$ and $\omega \rightarrow e^+e^-\pi^0$ were subtracted. The result of the model calculation considering the in-media modification for the (a) C and (b) Cu targets, together with (c) the fit result with the ρ - ω interference for the Cu target. The solid lines show the best-fit results. In (a) and (b), the shapes of $\omega \rightarrow e^+e^-$ (dotted) and $\rho \rightarrow e^+e^-$ (dash-dotted) were modified according to the model using the formula $m(\rho)/m(0) = 1 - k(\rho/\rho_0)$ with $k = 0.092$. In (c), the solid line shows the ρ - ω interfering shape with the $\rho/\omega = 0.64$ and the interference angle = 2.8 radian. The dotted line is the fit result with the typical values of the ρ/ω ratio = 1.0 and the angle = 2.0 radian [14].

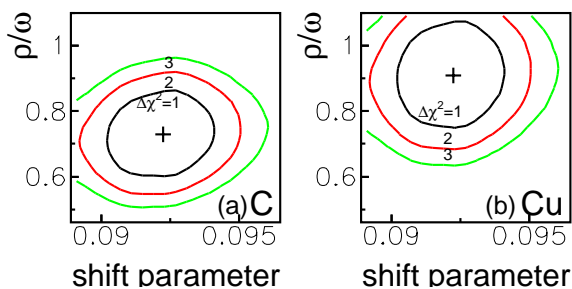


FIG. 3: Confidence ellipsoids for the shift parameter k (see text), and the production ratio ρ/ω , for the (a) C and (b) Cu targets. The step of each ellipsoid corresponds to $\Delta\chi^2=1$. The best fit point is indicated by the cross.

of excess was evaluated by subtracting the amplitude for the fit function from the data, in the range of 0.6 to $0.76\text{GeV}/c^2$. The obtained ratios of the excess to the ω peak in the acceptance are estimated to be 0.40 ± 0.04 and 0.40 ± 0.04 for the C and Cu targets, respectively. The obtained yields of each resonance and the excess are given in Table I. This procedure determines the ratio of ρ to ω , provided that they follow the relativistic Breit-Wigner distribution without any mass modification. After the acceptance correction, the 95% C.L. allowed parameter regions are obtained as $\rho/\omega < 0.15$ and $\rho/\omega < 0.31$ for C and Cu targets, respectively. The systematic errors arises from the uncertainty of the background estimation, which amount to 0.09 and 0.21 for the C and Cu targets, respectively. The obtained ρ/ω ratios are much smaller than unity, as was previously measured in pp interactions at the same energy [17]. A possible explanation is that most of the ρ are decaying inside the nuclei due to their short lifetime; their mass is modified in nuclear media

and contribute to the excess.

A comparison has been done for the data with a model considering the in-medium mass modification. In this model, the mass decreases linearly as a function of the density ρ , in the following relation: $m(\rho)/m(0) \simeq 1 - k(\rho/\rho_0)$ [5, 6]. The parameter k was expected to be $16 \pm 6\%$ for ρ and ω meson, where ρ_0 is the normal nuclear density [6]. The pole mass was modified by the above formula according to the density at the decay point. The decay-width modification was neglected. A Woods-Saxon shape was used for the nuclear density distribution; $\rho/\rho_0 \propto (1 + \exp((r-R)/\tau))^{-1}$, where $R = 2.3$ and 4.1 fm, $\tau = 0.57$ and 0.50 fm for the C and Cu targets, respectively. We assumed that the vector mesons were generated at the surface of an incident hemisphere of the target nucleus. This assumption is reasonable, since we have observed the mass-number dependence of the ω production cross section as $\sigma(A) \propto A^{2/3}$ [18]. This model predicts that the probabilities of ρ meson decays inside a nucleus are 46% and 61% for the C and Cu targets, respectively, while those of ω are 5% and 9%.

Based on the model, we modified the shapes of ρ and ω , by introducing the shift parameter k which is common for the C and Cu targets. We fit again the entire mass region of Fig.1 using the same procedure as before. The fit results, after subtracting the combinatorial background and the shapes of $\eta \rightarrow e^+e^-\gamma$ and $\omega \rightarrow e^+e^-\pi^0$ are shown in Fig.2(a) and (b). The spectra for both C and Cu targets can be reproduced quite well by this model. Confidence ellipsoids for the shift parameter k , and the ρ/ω ratio are also shown in Fig.3.

We obtained the shift parameter of $k = 0.092 \pm 0.002$. The best-fit values of the ρ/ω ratio are 0.7 ± 0.1 and 0.9 ± 0.2 for the C and Cu targets, respectively. Please

note that here the yield of ρ and ω includes both free decays and in-medium decays. It is concluded that the observed modification can be understood with the model in which the masses of the ρ and ω mesons decrease by 9% at the normal nuclear density. This value is consistent with the theoretical prediction [6].

We have neglected in-media mass broadening, which is theoretically predicted in [19, 20, 21, 22] and well summarized in [23, 24], since it appears that such width broadening of ρ and ω , which increases the yield of the high-mass tail, does not fit our data [29].

It is suggested that the $\rho - \omega$ interference is a possible explanation of the observed spectral modification [14]. Such possibility has been inspected by fitting the data with the interfering shape, which depends on the production ratio ρ/ω , and the interference angle θ [25]. We scanned the ρ/ω ratio from 0.2 to 2.6, and θ from 0.0 to 3.6 radian. It turned out that the fit was unsuccessful for any combination in the scanned regions, and rejected at 99.9% C.L. Around the suggested interference angle, 2 radian [14], the minimum χ^2 was found when θ was 2.8 and the ρ/ω ratio was 0.64. This result is shown in Fig.2(c), together with the curve for $\theta = 2.0$ radian and the ρ/ω ratio = 1.0 as a reference.

In summary, we have observed the excess over the known hadronic sources on the low-mass side of the ω meson peak in the e^+e^- invariant mass spectra. This demonstrates the spectral-shape modification of ρ and ω mesons in nuclear matter. Without the mass modification of hadrons, the obtained ρ/ω ratio, which is consistent with zero, contradicts to the known ρ/ω ratio at this energy. A possible explanation is that most of the ρ mesons decay inside the nucleus, and contribute to the excess. The observed excess is understood by the model in which the mass of ρ/ω meson decreases by 9% at the normal nuclear density, whereas the $\rho - \omega$ interference can not explain the data.

We would like to thank Prof. T. Hatsuda for helpful discussions. We greatly acknowledge all the staff members of KEK-PS, especially the beam channel group for their helpful support. This work was partly funded by the Japan Society for the Promotion of Science, RIKEN Special Postdoctoral Researchers Program and a Grant-in-Aid for Scientific Research from the Japan Ministry of Education, Culture, Sports, Science and Technology (MEXT). Finally, we also thank the staff members of RIKEN Super Combined Cluster system and RIKEN-CCJ.

* Electronic address: naruki@nh.scphys.kyoto-u.ac.jp

† Present Address: ICEPP, University of Tokyo, 7-3-1 Hongo, Tokyo 113-0033, Japan

- ‡ Present Address: Physics Department, Graduate School of Science, Tohoku University, Sendai 980-8578, Japan
- § Present Address: Division of Quantum Beam Material Science, Kyoto University Research Reactor Institute, Kumatori-cho, Sennan-gun, Osaka 590-0494, Japan
- ¶ Present Address: Japan Atomic Energy Research Institute, Tokai, Ibaraki 319-1195, Japan.
- ** Present Address: Faculty of Science and Technology, Tokyo University of Science, 2641 Yamazaki, Noda, Chiba 278-8510, Japan
- [1] T. Hatsuda and T. Kunihiro, Phys. Rept. **247**, 221 (1994).
- [2] G. E. Brown and M. Rho, Phys. Rept. **269**, 333 (1996).
- [3] G. E. Brown and M. Rho, Phys. Rev. Lett. **66**, 2720 (1991).
- [4] G. E. Brown and M. Rho, Phys. Rept. **363**, 85 (2002).
- [5] T. Hatsuda and S. H. Lee, Phys. Rev. C **46**, R34 (1992).
- [6] T. Hatsuda, S. H. Lee, and H. Shiomi, Phys. Rev. C **52**, 3364 (1995).
- [7] K. Ozawa *et al.*, Phys. Rev. Lett. **86**, 5019 (2001).
- [8] G. Agakichiev *et al.*, Eur. Phys. J. **C4**, 231 (1998).
- [9] J. Adams *et al.*, Phys. Rev. Lett. **92**, 092301 (2004).
- [10] G. M. Huber *et al.* (TAGX Collaboration), Phys. Rev. C **68**, 065202 (2003).
- [11] D. Trnka *et al.* (CBELSA/TAPS Collaboration), Phys. Rev. Lett. **94**, 192303 (2005).
- [12] M. Sekimoto *et al.*, Nucl. Inst. & Meth. **A 516**, 390 (2004).
- [13] S. Agostinelli *et al.* (GEANT4 Collaboration), Nucl. Inst. & Meth. **A 506**, 250 (2003).
- [14] R. Veenhof, in *proceedings of the 21st Winter Workshop on Nuclear Dynamics* (2005), URL http://www.star.bnl.gov/~panitkin/Breck_05/.
- [15] Y. Nara *et al.*, Phys. Rev. C **61**, 024901 (1999).
- [16] K. Hagiwara *et al.*, Phys. Rev. D **66**, 010001 (2002).
- [17] V. Blobel *et al.*, Phys. Lett. B **48**, 73 (1974).
- [18] T. Tabaru *et al.* (KEK-PS E325 Collaboration), (in preparation).
- [19] M. Asakawa, C. M. Ko, P. Levai, and X. J. Qiu, Phys. Rev. C **46**, R1159 (1992).
- [20] M. Herrmann, B. L. Friman, and W. Norenberg, Nucl. Phys. A **560**, 411 (1993).
- [21] F. Klingl, N. Kaiser, and W. Weise, Nucl. Phys. A **624**, 527 (1997).
- [22] W. Peters, M. Post, H. Lenske, S. Leupold, and U. Mosel, Nucl. Phys. A **632**, 109 (1998).
- [23] R. Rapp and J. Wambach, Adv. Nucl. Phys. **25**, 1 (2000).
- [24] M. Post, S. Leupold, and U. Mosel, Nucl. Phys. A **741**, 81 (2004).
- [25] D. Horn, Phys. Rev. D **1**, 1421 (1970).
- [26] G. Gounaris and J. Sakurai, Phys. Rev. Lett. **21**, 244 (1968).
- [27] G. Agakichiev *et al.* (CERES Collaboration) (2005), nucl-ex/0506002.
- [28] We have also examined the Gounaris-Sakurai shape [26] and the relativistic Breit-Wigner shape multiplied by the Boltzmann factor [27]. These shapes do not reproduce the data at C.L.99.9%.
- [29] Here we assumed that the width broadening is proportional to the density, the fit results actually favored the zero-broadening case.